Metabolic Engineering Communications 2 (2015) 124–131

Contents lists available at ScienceDirect

Metabolic Engineering Communications

journal homepage: www.elsevier.com/locate/mec

Redistribution of metabolic fluxes in *Chlorella protothecoides* by variation of media nitrogen concentration

Saratram Gopalakrishnan, Jordan Baker, Linda Kristoffersen, Michael J. Betenbaugh *

Johns Hopkins University, Department of Chemical and Biomolecular Engineering, 3400 N. Charles St., Maryland Hall 221, Baltimore, MD 21218, USA

ARTICLE INFO

Article history:
Received 2 April 2015
Received in revised form
30 August 2015
Accepted 30 September 2015
Available online 3 October 2015

Keywords:
Microalgae
Biofuels
Chlorella
MFA
EMU algorithm

ABSTRACT

In this study, the Elementary Metabolite Unit (EMU) algorithm was employed to calculate intracellular fluxes for *Chlorella protothecoides* using previously generated growth and mass spec data. While the flux through glycolysis remained relatively constant, the pentose phosphate pathway (PPP) flux increased from 3% to 20% of the glucose uptake during nitrogen-limited growth. The TCA cycle flux decreased from 94% to 38% during nitrogen-limited growth while the flux of acetyl-CoA into lipids increased from 58% to 109% of the glucose uptake, increasing total lipid accumulation. Phosphoenolpyruvate carboxylase (PEPCase) activity was higher during nitrogen-sufficient growth. The glyoxylate shunt was found to be partially active in both cases, indicating the nutrient nature has an impact on flux distribution. It was found that the total NADPH supply within the cell remained almost constant under both conditions. In summary, algal cells substantially reorganize their metabolism during the switch from carbon-limited (nitrogen-sufficient) to nitrogen-limited (carbon-sufficient) growth.
© 2015 The Authors. Published by Elsevier B.V. International Metabolic Engineering Society. This is an open access article under the CC BY-NC-ND license (http://creativecommons.org/licenses/by-nc-nd/4.0/).

1. Introduction

Over the last 50 years, algae have been utilized to produce a wide range of valuable commercial products (Rosenberg et al., 2011). However, recently, there has been particular interest in algae derived products as nutraceuticals and biofuels (Schmidt et al., 2010). Compared to other fuel sources, biofuels are renewable, non-toxic, and considered environmentally friendly (Miao and Wu, 2006). Due to the opportunities in algae biofuel production and the increased need for alternative energy, considerable attempts are being undertaken to optimize production of lipids and other biofuel precursors in microalgae. Commonly used microalgae strains for commercial applications include *Chlorella*, *Chamydomonas*, *Haematococcus* and *Dunaliella* (Rosenberg et al., 2011). *Chlorella protothecoides*, in particular, has been shown to produce high amounts of lipid precursors to biofuels in comparison to other strains (Miao and Wu, 2006). When algae cells are cultivated under nitrogen-limited conditions, the rate of lipid production has shown to increase compared to cultivation under nitrogen-sufficient growth. This is believed to be a survival mechanism as the accumulated lipids serve as energy storage when the cell is under stress (Rosenberg et al., 2008). Nitrogen limitation can increase production of lipids, but decreases the growth rate. *C. protothecoides* grown heterotrophically have yielded as much as 53% of its dry weight in lipids, typically stored as oil droplets in the cells, while photoautotrophic growth resulted in only 14% of its dry weight as lipids (Miao and Wu, 2006). The high production capability makes *C. protothecoides* a good candidate for an alternative fuel source. In an attempt to address this issue, growth studies using 13-C labeling have been performed to better understand metabolite flows within the cell in various growth conditions (Xiong et al., 2010).

Metabolic flux analysis (MFA) is a powerful tool that can provide details about all metabolic fluxes within a microorganism using stoichiometric constraints and radiolabeled tracers (Wiechert, 2001). The accuracy and methods of MFA have advanced significantly and is today based on stable-isotope labeling experiments and analysis of MS data for distributions of cellular metabolites (Antoniewicz et al., 2007b). At steady state, the resulting labeling pattern of each metabolic intermediate is fully and uniquely determined by the intracellular fluxes of the cell. Mathematical models relating network fluxes and mass isotopomer abundance from MS data in metabolic intermediates can facilitate this analysis (Antoniewicz et al., 2007b). Few studies have provided comprehensive and accurate flux models for algae cells. In particular, MFA using a skeletal representation of central metabolism, based on GC–MS-derived amino acid labeling patterns (Xiong et al., 2010), has revealed the re-routing of flux through the pentose phosphate pathway upon nitrogen starvation. However, we wanted to explore the role of glycine as a dual carbon and nitrogen source. Furthermore, a model that considered additional

* Corresponding author.
E-mail addresses: sgopala9@jhu.edu (S. Gopalakrishnan), jbaker66@jhu.edu (J. Baker), infinew@gmail.com (L. Kristoffersen), beten@jhu.edu (M.J. Betenbaugh).

http://dx.doi.org/10.1016/j.meteno.2015.09.004
2214-0301/© 2015 The Authors. Published by Elsevier B.V. International Metabolic Engineering Society. This is an open access article under the CC BY-NC-ND license (http://creativecommons.org/licenses/by-nc-nd/4.0/).

sources of NADPH, such as the chloroplastic transhydrogenase (Chopowick and Israelstam, 1971) that can alter the predicted fluxes through central metabolism (Bonarius et al., 1998), would be worthwhile. These differences warranted a further analysis of the generated GC–MS labeling data in order to obtain a more complete picture of the flux distribution and metabolic response of central metabolism to shift in nutrient limitation.

Hence, we have re-evaluated the reaction network of this *C. protothecoides* using previously generated amino acid labeling data and an expanded metabolic model in order to elucidate the driving forces behind the changes in metabolism during nitrogen-rich and nitrogen-limited growth conditions. This knowledge will enable researchers to further optimize growth and lipid production by understanding how the intracellular metabolism changes as a result of MFA analysis. After decomposing the network using the Elementary Metabolite Units (EMU) algorithm, fluxes were estimated by minimizing the variance-weighted sum of squares of deviation from experimentally observed labeling distributions (Antoniewicz et al., 2007a). This analysis indicated an increased dependence on the pentose phosphate pathway for generating NADPH following the shift from glucose to nitrogen-limited growth in order to meet the demands for increased lipid production, in conjunction with a reduced TCA cycle and glyoxylate shunt flux. Interestingly, the glyoxylate shunt was found to be partially active in both growth conditions to enable glycine incorporation into central metabolism. We also found that the total intracellular NADPH production remained relatively constant during both growth conditions.

2. Materials and methods

2.1. Description of the model

A one-compartment metabolic model for *C. protothecoides*, strain 0710, originally obtained from the Culture Collection of Alga at the University of Texas in Austin, grown heterotrophically on glucose and glycine was constructed consisting of glycolysis, pentose phosphate pathway, TCA cycle, glyoxylate shunt, and all of the amino acid biosynthetic pathways. Supplementary Tables S2 and S3 provides the complete list of reactions and metabolites included in the metabolic model of *C. protothecoides*. The primary carbon source, glucose, is metabolized via the central carbon metabolic pathways, ultimately producing the precursors for biomass production. The supplied nitrogen source is glycine, which is also a carbon source. Sulfur is incorporated into the two amino acids, cysteine and methionine. Phosphate is used for ATP synthesis and energy production. Incorporated oxygen is assumed to be used exclusively for oxidative phosphorylation.

The model also includes cofactor and energy components, which address the overall energy demand for biosynthetic processes. A general ATP hydrolysis reaction is included to account for all ATP requirements over the quantifiable growth-associated maintenance (GAM) of 15.58 mmol/gdw during nitrogen-sufficient growth and 20.36 mmol/gdw during nitrogen-limited growth. This difference arises from changes in biomass composition in the form of increased lipid content and decreased protein content upon nitrogen starvation. Quantifiable ATP costs include biosynthesis and polymerization of macromolecules such as proteins, DNA, RNA, lipids, and carbohydrates. Additional costs covered by the ATP hydrolysis reaction include protein activation, futile cycles, non-growth associated maintenance, and unquantifiable GAM costs.

The reversible transfer of hydride between NAD and NADH and NADP and NADPH has also been included in the model to account for the activities of the mitochondrial and chloroplastic nicotinamide nucleotide transhydrogenases (Krawetz and Israelstam, 1978) and the presence of isozymes using different cofactors. The lack of compartmentalization prevents the distinction between the various compartmental cofactor pools. Since intercompartment cofactor shuttling does not generate or consume NADH or NADPH, information about total NADH, NADPH, and ATP production within the cell can be reliably extracted from the obtained flux distribution. Furthermore, relaxation of cofactor constraints using transhydrogenase and an ATP sink prevents any bias arising from incorrectly included cofactor balances (Bonarius et al., 1998).

The non-oxidative pentose phosphate pathway consists of three reactions following the bisubstrate ping-pong mechanism (Nilsson et al., 1997; Jia et al., 1997), with three possible group donors and three possible acceptors. In order to capture all possible carbon transitions accurately, they are modeled as half-reactions (Kleijn et al., 2005).

Synthesis of glutamate is modeled using the GS:GOGAT system. Aspartate, alanine, and serine are synthesized by transamination reactions with glutamate as the amino group donor. Glycine is taken up from the medium and converted to glyoxylate by a glyoxylate aminotransferase enzyme. The synthesis of the remaining amino acids is assumed to be the same as in bacteria. The synthesis of lipids is described in terms of acetyl-CoA and energy terms NADPH and ATP (Stephanopoulos et al., 1998). The lipid profile of *C. protothecoides* has been described previously (Xiong et al., 2010). Using this information, a stoichiometric equation for synthesis of 1 g lipids has been calculated.

The defined biomass equations describe the formation of 1 g biomass in terms of macromolecules (DNA, RNA, proteins, lipids, and carbohydrates). Lipids are assumed to be exclusively diacylglycerols (DAGs) based on the previously described biomass equation for *C. protothecoides* (Xiong et al., 2010). The composition of fatty acids and amino acids used in the model for this strain have been previously defined (Xiong et al., 2010). Carbohydrates are modeled in terms of hexose monomer units (molecular weightt 162 g/mole). DNA and RNA are modeled in terms of nucleotide monophosphates (NMPs and dNMPs), the precursor and energy requirements for which have been defined previously (Stephanopoulos et al., 1998).

2.2. Raw data

The experimental data used in our model was kindly obtained from a previous study assessing the impact of nitrogen starvation on *C. protothecoides* (Xiong et al., 2010). Glucose and glycine were used as the carbon and nitrogen source respectively. 10% of the supplied glucose was labeled with U-13 C. The growth rates and the glucose consumption rates were measured, and the amino acid mass spectra was obtained using GC–MS analysis. Using this data, a comprehensive model describing the metabolic network of *C. protothecoides* under nitrogen-sufficient and nitrogen-limited conditions was constructed in the current study.

2.3. Mass spectrometry fragment selection

To improve accuracy during metabolic flux analysis, error related to the GC–MS data is minimized. Amino acid fragments were selected for analysis based on accuracy and precision criteria described in a previous study (Antoniewicz et al., 2007a). Supplementary Table S1 provides details about which fragments were used in the flux model and which ones were rejected. Fragments were excluded from the analysis for two reasons: their absolute intensity was low, or the data resulted in negative fractions after correction for natural abundance.

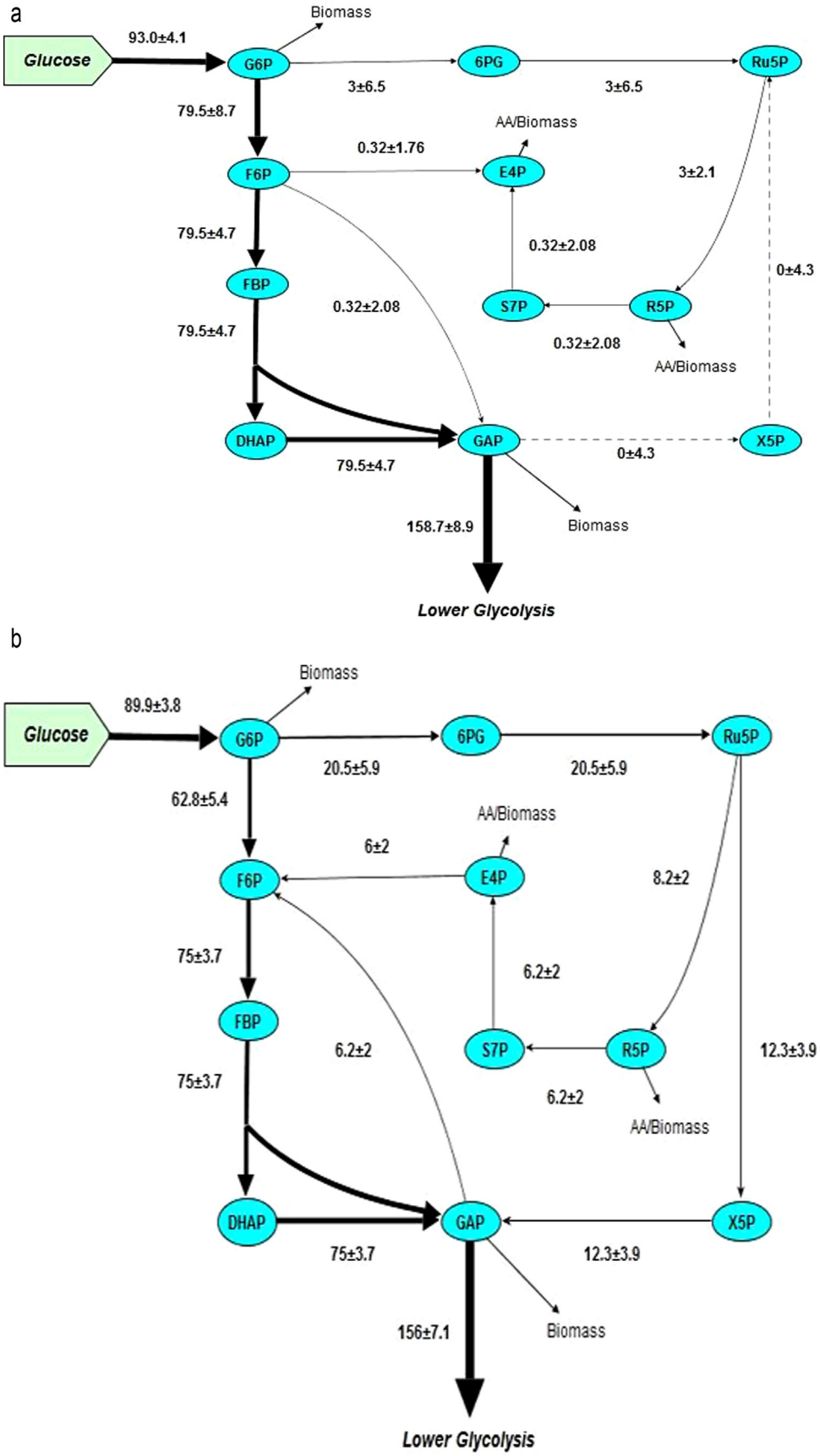

Fig. 1. PPP Flux. Fluxes (in % glucose uptake) through glycolysis and PPP during: (a) nitrogen-sufficient growth (left), and (b) nitrogen-limited growth (right).

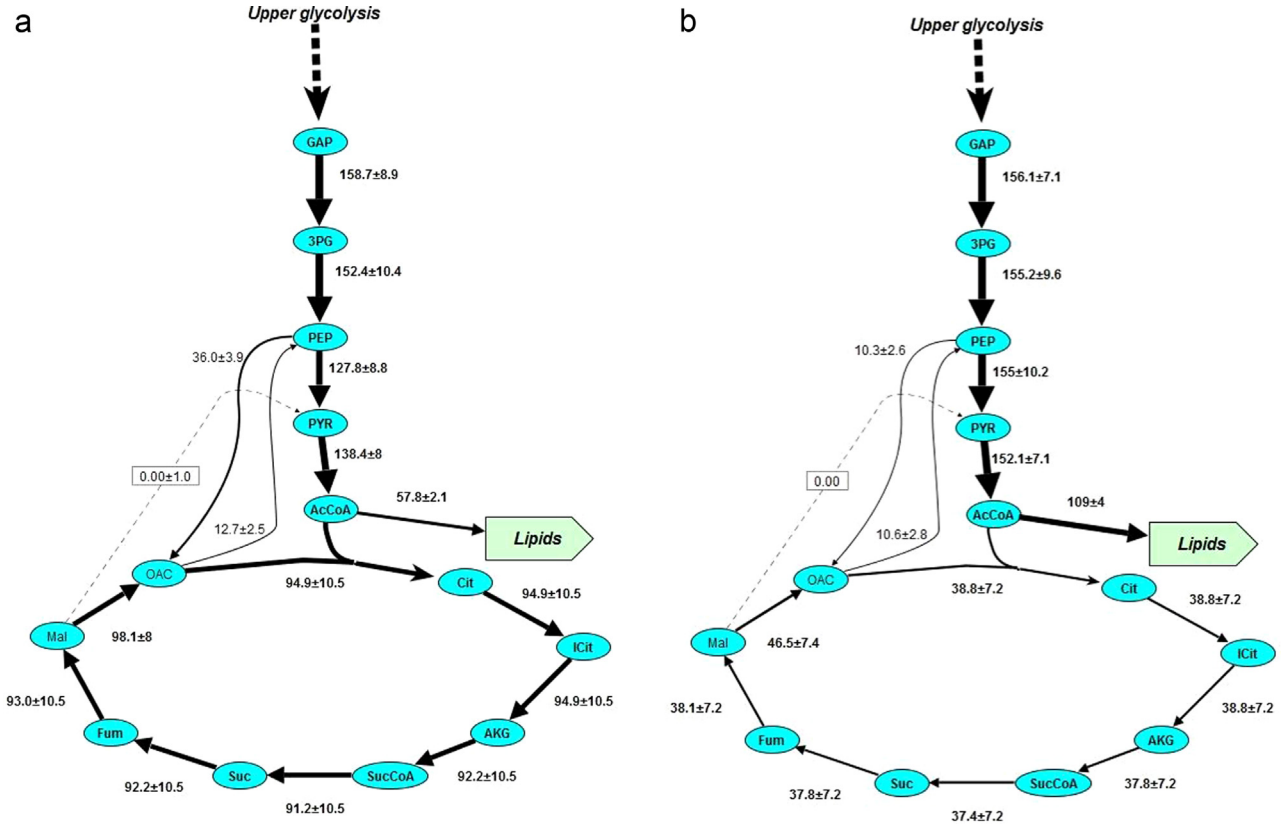

Fig. 2. Lower Glycolysis and TCA Cycle Fluxes. Fluxes (in % glucose uptake with their corresponding errors) through lower glycolysis and TCA cycle during: (a) nitrogen-sufficient growth (left), and (b) nitrogen-limited growth (right).

2.4. Estimation of intracellular fluxes

The EMU algorithm was used to calculate the intracellular fluxes using the above described model, growth and substrate consumption rates, and selected fragments (Antoniewicz et al., 2007a). The advantage of this method is that it uses only a limited number of atom balances, thereby greatly decreasing computation time. A software package, METRAN (Antoniewicz et al., 2007a, 2007b, 2006; Yoo et al., 2008), kindly provided by Professor Antoniewicz was used to estimate fluxes using the EMU algorithm. In addition to calculating fluxes, this software is also capable of determining the confidence intervals (Antoniewicz et al., 2006) for each estimated flux, which provides information on the uncertainties in flux estimation using experimental data measurement errors. Fluxes were estimated with and without including cofactor balances to assess the sensitivity of the obtained flux distribution to these additional constraints. The obtained fits remained identical with and without the inclusion of cofactor balances, rendering the obtained solution insensitive to these additional cofactor balances. This insensitivity to cofactor balances arises from the lack of an oxygen uptake measurement, which limits ATP, NADH and NADPH production. The best fits for the nitrogen-sufficient and nitrogen-limited growth conditions were found to be 88 and 84 with their maximum allowed sum of squares of residuals being 107 and 138, respectively.

3. Results

3.1. Glycolysis and pentose phosphate pathway

Shown in Fig. 1A and B are the fluxes through glycolysis and the pentose phosphate pathway during nitrogen-sufficient and nitrogen-limited growth, respectively. It is evident that the glycolysis pathway is favored over the pentose phosphate pathway (PPP) for glucose metabolism in nitrogen sufficient conditions. Nitrogen-limiting conditions showed an increased flux through the oxidative branch of the pentose phosphate pathway (20% of the glucose uptake compared to 3% in nitrogen-sufficient conditions). As a result of this, the flux through phosphoglucose isomerase (PGI) was higher in nitrogen-sufficient conditions (80% compared to 62% during nitrogen-limited growth). Since the Entner–Doudoroff pathway is absent in algae, the higher PPP flux increased the NADPH production from this pathway at the expense of one CO_2 per G6P metabolized via this pathway. This increased NADPH produced from this pathway was utilized for the production of lipids during nitrogen-limited growth conditions (see later section on NADPH).

A consequence of an increased flux through the oxidative PPP was the reversal of the direction of the non-oxidative branch of the pentose phosphate pathway. During nitrogen-limited growth, the flux through the oxidative pentose phosphate pathway is 20% of the glucose uptake rate, as compared to 3% during nitrogen-sufficient growth. During nitrogen-limited growth, the flux through the oxidative pentose phosphate pathway is more than the combined R5P and E4P demand of 0.31 mmol/gdw h and 0.05 mmol/gdw h, respectively, resulting in the production of excess pentose phosphates. These excess pentose sugars are metabolized via the non-oxidative pentose phosphate pathway to produce glycolytic intermediates, therefore shifting the direction of the pathway from the pentose pools towards glycolysis. During nitrogen-sufficient growth, the flux through the oxidative pentose phosphate pathway is a small value above the ribose demand making the direction of the non-oxidative away from glycolysis and towards E4P and R5P (Fig. 1).

3.2. TCA cycle and pyruvate metabolism

The flux through pyruvate dehydrogenase (Fig. 2) was higher during nitrogen-limited growth than during nitrogen-sufficient growth (152% vs. 138% of glucose uptake). Despite this, the flux through the TCA cycle during nitrogen-sufficient growth was significantly higher (94% vs. 39%). This is because more acetyl-CoA produced by this reaction was diverted towards lipid production in nitrogen-limited growth conditions than during nitrogen sufficient conditions (109% vs. 58%). The TCA cycle served two purposes: production of biomass precursors and production of energy in the form of NADPH and ATP. During nitrogen-sufficient growth, the higher TCA cycle flux favors carbon skeleton generation for improved carbon and nitrogen assimilation into protein synthesis. It also provides reducing equivalents to meet growth demands. During nitrogen-limited growth, the carbon skeleton and energy demands for growth are decreased. Therefore, the fluxes around acetyl-CoA are readjusted to favor enhanced lipid production (109% vs. 58%).

Among the anaplerotic reactions, malic enzyme was found to be inactive in both cases, Phosphoenolpyruvate Carboxykinase (PEPCk) activity relative to glucose uptake was similar in both cases, and Phosphoenolpyruvate Carboxylase (PEPCase) was higher during nitrogen-sufficient growth (36% compared to 10% of the glucose uptake). PEPCk and PEPCase provide a means of reversible conversion between glycolytic and TCA intermediates. A higher PEPCase flux compared to PEPCk indicates a net flow of metabolites from glycolysis to the TCA cycle. With constant PEPCk flux under both growth conditions, a higher PEPCase flux during nitrogen sufficient growth provides a means to replenish TCA metabolites drained away for amino acid biosynthesis (AKG for Glu, Gln, Pro, and Arg biosynthesis and OAA for Asp, Asn, Thr, Lys, and Met biosynthesis). Both iso-forms of malic enzyme (ME) were predicted to be inactive, indicating that NADPH is produced from other pathways within the network. Malic enzyme (ME) only alters alanine labeling distribution whereas PEPCK alters the labeling distribution of all amino acids produced using glycolytic intermediates, making the labeling distribution of amino acids more sensitive to flux through PEPCK compared to ME.

3.2.1. Flux of acetyl-CoA into lipids

The flux of acetyl-CoA into lipids, relative to glucose uptake, was higher during nitrogen-limited growth (57% vs. 109%). Previous studies have shown increased lipid production in response to nitrogen starvation (Sheehan et al., 1998). Acetyl-CoA is produced by the oxidation of pyruvate by pyruvate dehydrogenase, which links glycolysis to the TCA cycle. The distribution of acetyl-CoA flux across various pathways during nitrogen-sufficient and nitrogen-limited growth is shown in Fig. 3. Acetyl-CoA can be either metabolized via the TCA cycle to produce energy, or used for fatty acid biosynthesis. Acetyl-CoA is also used for the synthesis of malate in the glyoxylate shunt, and for leucine and fatty acid synthesis. The flux through each of these pathways is dictated by the availability of acetyl-CoA and energy. When nitrogen is abundant, there is a large demand for TCA metabolites (AKG and OAA) for amino acid synthesis. The large energy pool is also rapidly depleted due to increased energy demand for growth. As a result, the flux through the TCA cycle is higher, amounting to 60% of the total acetyl-CoA consumption flux. The flux of acetyl-CoA into lipids (36% of the total acetyl-CoA) is adjusted such that the minimum lipid requirement of the cell is met. During nitrogen-limited growth, there are some significant shifts in this distribution. Protein content decreases during nitrogen starvation. As a result, demand for amino acid precursors decreases. In this state, the TCA cycle's primary role is energy production. The presence of excess acetyl-CoA and energy, among other possible contributions,

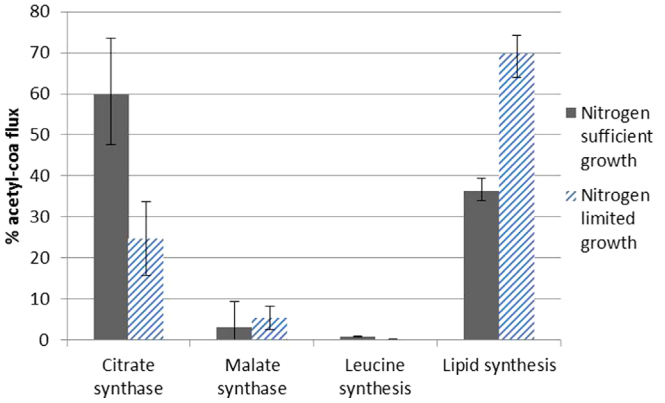

Fig. 3. Acetyl-CoA Flux. Acetyl-CoA distribution across various pathways during nitrogen sufficient (■) and nitrogen limited (⁒) growth.

favors lipid biosynthesis. The fluxes around acetyl-CoA are adjusted to account for these factors by channeling more acetyl-CoA into lipids (70%) and much less into the TCA cycle (25%). The metabolic network during nitrogen-limited growth is readjusted to maximize lipid production while optimizing energy usage within the cell.

3.2.2. Glycine metabolism and the glyoxylate shunt

Glycine was the primary nitrogen source to the microalga, and glycine metabolism changed significantly in the two cases (Fig. 4). The raw MS data revealed that most of the glycine and serine was unlabeled, indicating most of the intracellular glycine was taken up from the extracellular medium. The labeled fraction comes from interactions with glycolysis through the serine biosynthesis pathway and serine-hydroxymethyltransferase (SHMT). The glycine uptake rate, relative to glucose, decreases from 19% during nitrogen-sufficient growth to 6% during nitrogen-limited growth, following a shift in the limiting nutrient from glucose to glycine. As expected, the flux of glycine into the cell decreased significantly during nitrogen-limited growth. During nitrogen-sufficient growth, most of the glycine was metabolized by glycine dehydrogenase, producing a one-carbon unit, Methylenetetrahydrofolate (MEETHF), which then recombined with glycine to produce serine through serine hydroxymethyltransferase (SHMT) (Fig. 4). Some of the glycine underwent transamination by alanine-glyoxylate transaminase to produce glyoxylate, which fed into the glyoxylate shunt. The rest was primarily incorporated into proteins. During nitrogen-limited growth, glycine dehydrogenase activity decreased considerably, and the majority of glycine fed the glyoxylate shunt. Indeed, there was an increase in glycine channeling into the glyoxylate shunt even though less overall glycine was utilized. An interesting consequence of using glycine as the nitrogen source was a partially active glyoxylate shunt. Isocitrate lyase, the first reaction of the glyoxylate shunt, was inactive in both cases. As a result of this, isocitrate does not contribute to malate formation via the glyoxylate shunt. This explains the absence of intact C1-C2 or C3-C4 connections observed in the previous study (Xiong et al., 2010). The second reaction, malate synthase, was calculated to be active in both cases. A partially active glyoxylate shunt provides the means to assimilate the carbon contained within the nitrogen source, glycine.

Degradation of glycine by glycine dehydrogenase produces free ammonia, which utilizes one ATP and one NADPH to be re-incorporated. The reduction of glycine dehydrogenase activity during nitrogen-limited growth is likely a direct consequence of decreased glycine uptake and the need to retain incorporated nitrogen. Glycine catabolism via transaminases costs no energy and produces glyoxylate, which feeds excess carbon skeletons from

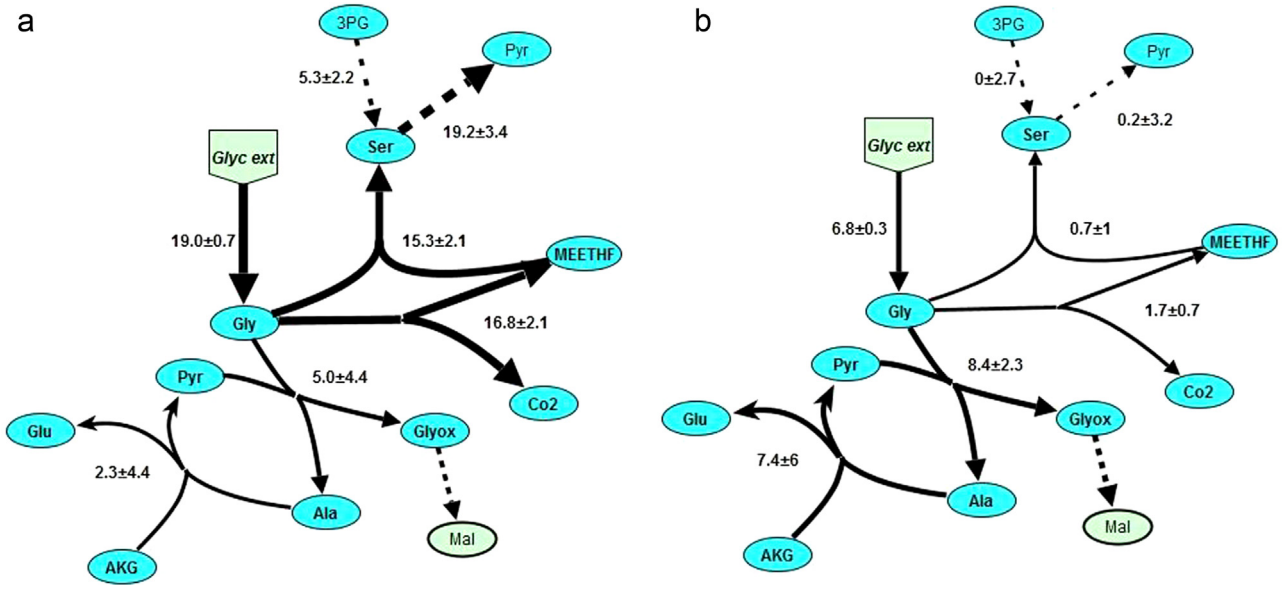

Fig. 4. Glycine Metabolism. Glycine metabolism during: (A) nitrogen-sufficient growth (left), and (B) nitrogen-limited growth (right).

glycine directly into the glyoxylate shunt. It is likely that the cell favors degradation by transaminases over glycine dehydrogenase to minimize the usage of reducing equivalents, which can instead, be used for lipid biosynthesis. Thus, glyoxylate is a node and not an intermediate of a linear pathway, and therefore, partial activity of a previously assumed linear pathway is possible. Algal metabolism using glycine clearly indicates that the nature of nitrogen source can have a profound impact on the labeling patterns of intracellular metabolites and metabolite flows.

3.2.3. *NADPH sources and allocation within the cell*

The oxidative pentose phosphate pathway (OxPPP), isocitrate dehydrogenase (IDH1), malic enzyme (ME), and transhydrogenase (TH) are the known sources of NADPH within the cell. The contribution of NADPH from each of these sources was estimated and is shown in Fig. 5. Transhydrogenase mechanisms (both mitochondrial and chloroplastic) were found to be a significant source of NADPH in both growth conditions. IDH1 in the TCA cycle was a prominent source in nitrogen-sufficient conditions. Under nitrogen-limited conditions, most of the acetyl-CoA was used for lipid synthesis (Fig. 2). As a result, flux of carbon into the TCA cycle greatly decreased, thereby decreasing the contribution of IDH1 to the total NADPH pool. Additional NADPH is produced by the oxidative pentose phosphate pathway, which was found to have very limited activity during nitrogen-sufficient growth conditions, but increased during nitrogen-limited growth. Since the Entner–Doudoroff pathway is absent in algae, the oxidative pentose phosphate pathway produces 2 mol of NADPH and one CO_2 per mole of glucose metabolized. The disadvantage of using this pathway is that carbons are lost as carbon dioxide, which is energetically expensive to re-incorporate. During nitrogen-limited growth, conservation of carbons is not a priority, therefore, this pathway contributed to the total NADPH pool.

An interesting observation was that total NADPH produced by the cell under both growth conditions remained constant. The NADPH requirement calculated for synthesis of DNA, RNA, proteins and lipids is 6.3 mmol, 2.2 mmol, 16.2 mmol, and 56.3 mmol respectively. As shown in Fig. 6, the total NADPH produced by the microalgae during both growth conditions remains approximately constant, even though the cells have different compositions. Interestingly, it is known that NADPH levels in cells are tightly controlled (Pollak et al., 2007). The enzymes affected by the NADPH/$NADP^+$ ratio are activated by $NADP^+$ and inhibited by NADPH (Singh et al., 2012). From a flux balance analysis perspective (Varma and Palsson, 1994), if NADPH is assumed to be a balanced metabolite (Bonarius et al., 1997; Savinell and Palsson, 1992), the flux of NADPH into biomass synthesis must equal total NADPH production inside the cell. The constant total NADPH flux in both cases gives us an insight into a possible additional

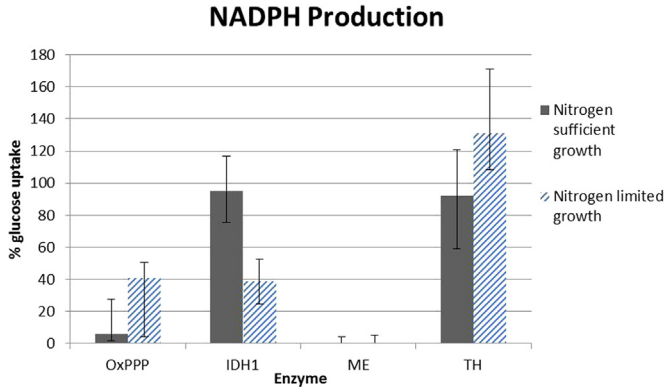

Fig. 5. NADPH production. Contribution of different enzymes to the NADPH pool during nitrogen sufficient (■) and nitrogen limited (▨) growth. The error bars depict the width of the 95% confidence interval.

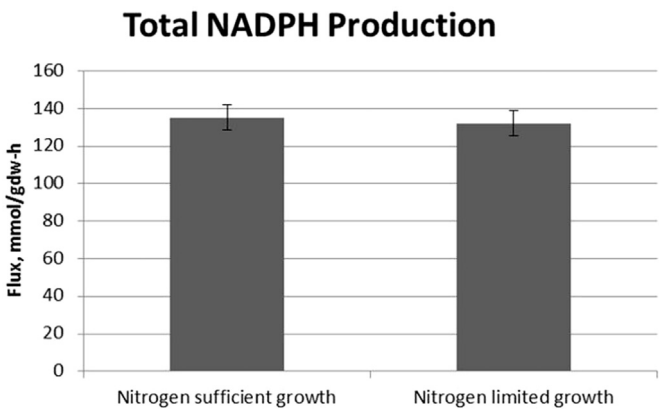

Fig. 6. Total NADPH Production. Total NADPH flux inside the cell.

metabolic constraint that affects overall cellular metabolism. This phenomenon has been seen before in *C. glutamicum* which overproduces lysine (Wittmann and Heinzle, 2002). It was seen that while NADPH demand increased for strains with enhanced lysine production, the supply of NADPH remained relatively constant in all cases. Further evaluation will be needed to verify whether other microalgae species also adhere to this constraint during various growth conditions.

4. Discussion and conclusion

Analysis of 13-C tracer data of *C. protothecoides* has revealed that the nature of nutrient sources plays a critical role in determining fluxes through different pathways. Glycine provided in the extracellular growth medium as a nitrogen source can either be degraded via glycine dehydrogenase for amino acids, or channeled into the glyoxylate shunt for TCA intermediates. A partially active glyoxylate shunt indicates that the carbon from the supplied amino acid can be metabolized, and used for biosynthetic reactions. The flux through the pentose phosphate pathway can vary depending on the growth conditions to meet the intracellular precursor and NADPH demands. It was interesting to note that despite the previously reported heavy dependence on the pentose phosphate pathway (Xiong et al., 2010; Yang et al., 2000) it carried very little flux during nitrogen-sufficient growth conditions, similar to some non-photosynthetic plant tissues (Agrawal and Canvin, 1971). Under nitrogen-limited growth conditions, the increased PPP flux helps meet the increased NADPH demand for lipid biosynthesis.

NADP-Malic enzyme was previously reported to be the primary source of NADPH for fatty acid synthesis in oleaginous fungi (Holdsworth et al., 1988; Wynn et al., 1999; Ratledge, 2002). In plants, it is known to be a part of the CO_2 transport mechanism for the C4 and Crassulacean Acid Metabolism (CAM) photosynthetic pathways (Christopher and Holtum, 1996; Kanai and Edwards, 1973). However, we found that this reaction was inactive, which was consistent with the NMR analysis performed in earlier studies (Xiong et al., 2010). The identification of other localized sources of NADPH for fatty acid synthesis in *Chlorella* requires further investigation. PEPCase, along with NADP-malic enzyme form a transport system for CO_2 and NADPH in C4 and CAM plants. PEPCk is a part of the gluconeogenesis pathway and is used to synthesize glycolysis metabolites from TCA. PEPCase activity in the absence of photosynthesis indicated anaplerotic function. Together, PEPCk and PEPCase form a futile cycle, which serves to shuttle carbons between glycolysis and the TCA cycle.

The flexibility and stability of central carbon metabolism and maintenance of a constant NADPH supply within the cell provides a means of adaptation to nutrient starvation conditions. During nitrogen-limited growth, the flux through the TCA cycle decreased from 94% to 38% of the glucose uptake, while the flux of acetyl-CoA into lipids increased from 58% to 109% of the glucose uptake rate, likely due to the impact of nitrogen availability. This change also prompted a shift in the means for generating NADPH for cellular demands. The accumulation of lipids during nitrogen-sufficient growth is a strategy used by the cells to store excess carbon available as fatty acids, to be used later during carbon limiting conditions, since fatty acids can be metabolized and incorporated into the metabolic network through the glyoxylate shunt. The activity of PEPCase during heterotrophic growth implies an anaplerotic function of replenishing oxaloacetate for synthesis of growth precursors. The prediction of an inactive malic enzyme raises an interesting question on how the cell generates chloroplastic NADPH for macromolecule monomer biosynthesis. To answer this question, a more comprehensive model, comprised of multiple intracellular compartments, will be required. Such a model will highlight the function of redox transport mechanisms between different compartments. Thus, we have shown that 13-C tracer analysis can be applied to microalgae to provide insights for future bioprocess and metabolic engineering manipulations aimed at biofuel applications.

Conflict of interest

The authors declare that they have no conflict of interest.

Acknowledgments

We would like to thank Dr. Qingyu Wu of Tsinghua University for providing us the raw GC data of the algae under varying nitrogen conditions for us to perform the metabolic flux analysis. We would also like to thank Dr. Maciek Antoniewicz of the University of Delaware for providing us with help and support on the flux analysis and the software to perform the analysis. This work was supported in part by the National Science Foundation's (NSF) EFRI grant #NSF-EFRI-1332344.

Appendix A. Suplementary information

Supplementary data associated with this article can be found in the online version at http://dx.doi.org/10.1016/j.meteno.2015.09.004.

References

Agrawal, P.K., Canvin, D.T., 1971. Contribution of pentose phosphate pathway in developing castor bean endosperm. Canadian Journal of Botany 49, 267–272.
Antoniewicz, M.R., Kelleher, J.K., Stephanopoulos, G., 2006. Determination of confidence intervals of metabolic fluxes estimated from stable isotope measurements. Metab. Eng. 8 (4), 324–337. http://dx.doi.org/10.1016/j.ymben.2006.01.004.
Antoniewicz, M.R., Kelleher, J.K., Stephanopoulos, G., 2007a. Accurate assessment of amino acid mass isotopomer distributions for metabolic flux analysis. Anal. Chem. 79 (19), 7554–7559. http://dx.doi.org/10.1021/ac0708893.
Antoniewicz, M.R., Kelleher, J.K., Stephanopoulos, G., 2007b. Elementary metabolite units (EMU): a novel framework for modeling isotopic distributions. Metab. Eng. 9 (1), 68–86. http://dx.doi.org/10.1016/j.ymben.2006.09.001.
Bonarius, H.P.J., Schmid, G., Tramper, J., 1997. Flux analysis of underdetermined metabolic networks: the quest for the missing constraints. Trends Biotechnol. 15 (8), 308–314. http://dx.doi.org/10.1016/S0167-7799(97)01067-6.
Bonarius, H.P., Timmerarends, B., deGooijer, C.D., Tramper, J., 1998. Metabolite-balancing techniques vs. 13c tracer experiments to determine metabolic fluxes in hybridoma cells. Biotechnology and bioengineering 58, 258–262.
Chopowick, R., Israelstam, G.F., 1971. Pyridine nucleotide transhydrogenase from chlorella. Planta 101, 171–173.
Christopher, J.T., Holtum, J., 1996. Patterns of carbon partitioning in leaves of crassulacean acid metabolism species during deacidification. Plant Physiol. 112 (1), 393–399. http://dx.doi.org/10.1104/pp.112.1.393.
Holdsworth, J.E., Veenhuis, M., Ratledge, C., 1988. Enzyme activities in oleaginous yeasts accumulating and utilizing exogenous or endogenous lipids. J. Gen. Microbiol. 134 (11), 2907–2915. http://dx.doi.org/10.1099/00221287-134-11-2907.
Jia, J., Lindqvist, Y., Schneider, G., Schörken, U., Sprenger, G.A., 1997. Crystal structure of the reduced schiff-base intermediate complex of transaldolase B from escherichia coli: mechanistic implications for class I aldolases. Protein Sci. 6 (1), 119–124. http://dx.doi.org/10.1002/pro.5560060113.
Kanai, R., Edwards, G.E., 1973. Separation of mesophyll protoplasts and bundle sheath cells from maize leaves for photosynthetic studies. Plant Physiol. 51 (6), 1133–1137. http://dx.doi.org/10.1104/pp.51.6.1133.
Kleijn, R.J., van Winden, W.A., van Gulik, W.M., Heijnen, J.J., 2005. Revisiting the 13C-label distribution of the non-oxidative branch of the pentose phosphate pathway based upon kinetic and genetic evidence. FEBS J. 272 (19), 4970–4982. http://dx.doi.org/10.1111/j.1742-4658.2005.04907.x.
Krawetz, S.A., Israelstam, G.F., 1978. Kinetics of pyridine nucleotide transhydrogenase from *Chlorella*. Plant Sci. Lett. 12 (3–4), 323–326. http://dx.doi.org/10.1016/0304-4211(78)90085-8.
Miao, X., Wu, Q., 2006. Biodiesel production from heterotrophic microalgal oil.

Bioresour. Technol. 97 (6), 841–846. http://dx.doi.org/10.1016/j.biortech.2005.04.008.
Nilsson, U., Meshalkina, L., Lindqvist, Y., Schneider, G., 1997. Examination of substrate binding in thiamin diphosphate- dependent transketolase by protein crystallography and site-directed mutagenesis. J. Biol. Chem. 272 (3), 1864–1869. http://dx.doi.org/10.1074/jbc.272.3.1864.
Pollak, N., Dolle, C., Ziegler, M., 2007. The power to reduce: pyridine nucleotides—small molecules with a multitude of functions. Biochem. J. 402 (2), 205–218. http://dx.doi.org/10.1042/BJ20061638.
Ratledge, C., 2002. Regulation of lipid accumulation in oleaginous micro-organisms. Biochem. Soc. Trans. 30 (Pt 6), 1047–1050, doi: 10.1042/.
Rosenberg, J.N., Betenbaugh, M.J., Oyler, G.A., 2011. Biofuel's Engineering Process Technology.
Rosenberg, J.N., Oyler, G.A., Wilkinson, L., Betenbaugh, M.J., 2008. A green light for engineered algae: redirecting metabolism to fuel a biotechnology revolution. Curr. Opin. Biotechnol. 19 (5), 430–436. http://dx.doi.org/10.1016/j.copbio.2008.07.008.
Savinell, J.M., Palsson, B.O., 1992. Network analysis of intermediary metabolism using linear optimization. I. Development of mathematical formalism. J. Theor. Biol. 154 (4), 421–454.
Schmidt, B.J., Lin-Schmidt, X., Chamberlin, A., Salehi-Ashtiani, K., Papin, J.A., 2010. Metabolic systems analysis to advance algal biotechnology. Biotechnol. J. 5 (7), 660–670. http://dx.doi.org/10.1002/biot.201000129.
Singh, S., Anand, A., Srivastava, P.K., 2012. Regulation and properties of glucose-6-phosphate dehydrogenase: a review. Int. J. Plant Physiol. Biochem. 4 (1), 1–19.
Sheehan, J., Dunahay, T., Benemann, J., Roessler, P., 1998. A Look Back at the U.S. Department of Energy's Aquatic Species Program: Biodiesel from Algae. National Renewable Energy Laboratory, Golden, Colorado, TP-580-24190.
Stephanopoulos, G.N., Aristidou, A.A., Nielsen, J., 1998. Review of cellular metabolism (Chapter 2). In: Stephanopoulos, G.N., Aristidou, A.A., Nielsen, J. (Eds.), Metabolic Engineering. Academic Press, San Diego, pp. 21–79. http://dx.doi.org/10.1016/B978-012666260-3/50003-0.
Varma, A., Palsson, B.O., 1994. Metabolic flux balancing: basic concepts, scientific and practical use. Nat. Biotechnol. 12 (10), 994–998.
Wiechert, W., 2001. 13C metabolic flux analysis. Metab. Eng. 3 (3), 195–206. http://dx.doi.org/10.1006/mben.2001.0187.
Wittmann, C., Heinzle, E., 2002. Genealogy profiling through strain improvement by using metabolic network analysis: metabolic flux genealogy of several generations of lysine-producing corynebacteria. Appl. Environ. Microbiol. 68 (12), 5843–5859. http://dx.doi.org/10.1128/AEM.68.12.5843-5859.2002.
Wynn, J.P., Hamid, Ab.A., Ratledge, C., 1999. The role of malic enzyme in the regulation of lipid accumulation in filamentous fungi. Microbiology 145 (8), 1911–1917. http://dx.doi.org/10.1099/13500872-145-8-1911.
Xiong, W., Liu, L., Wu, C., Yang, C., Wu, Q., 2010. 13C-tracer and gas chromatography-mass spectrometry analyses reveal metabolic flux distribution in the oleaginous microalga Chlorella protothecoides. Plant Physiol. 154 (2), 1001–1011. http://dx.doi.org/10.1104/pp.110.158956.
Yang, C., Hua, Q., Shimizu, K., 2000. Energetics and carbon metabolism during growth of microalgal cells under photoautotrophic, mixotrophic and cyclic light-autotrophic/dark-heterotrophic conditions. Biochem. Eng. J. 6 (2), 87–102.
Yoo, H., Antoniewicz, M.R., Stephanopoulos, G., Kelleher, J.K., 2008. Quantifying reductive carboxylation flux of glutamine to lipid in a brown adipocyte cell line. J. Biol. Chem. 283 (30), 20621–20627. http://dx.doi.org/10.1074/jbc.M706494200.